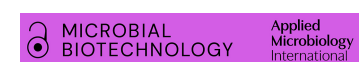
RESEARCH ARTICLE



Check for updates

Exploring engineered vesiculation by *Pseudomonas putida* KT2440 for natural product biosynthesis

Nora Lisa Bitzenhofer ¹
Andrea Jeanette Weiler ¹ Christian Eberlein ² Hermann J. Heipieper ²
Renu Batra-Safferling ³ Pia Sundermeyer ^{4,5} Thomas Heidler ^{4,5}
Carsten Sachse ^{4,5,6}
Thomke Belthle ^{9,10}
Anita Loeschcke ¹ [©]

Correspondence

Anita Loeschcke, Institute of Molecular Enzyme Technology, HHU Düsseldorf, Wilhelm-Johnen-Straße, 52428 Jülich, Germany

Email: a.loeschcke@fz-juelich.de

Funding information

Bundesministerium für Bildung und Forschung, Grant/Award Number: 031B0837A, 031B0852B, 031B085C and 161B0866A; Deutsche Forschungsgemeinschaft, Grant/ Award Number: Project ID 458090666 / CRC1535/1; European Regional Development Fund (EFRE), Grant/Award Number: 34.EFRE-0300095/1703F104

Abstract

Pseudomonas species have become promising cell factories for the production of natural products due to their inherent robustness. Although these bacteria have naturally evolved strategies to cope with different kinds of stress, many biotechnological applications benefit from engineering of optimised chassis strains with specially adapted tolerance traits. Here, we explored the formation of outer membrane vesicles (OMV) of Pseudomonas putida KT2440. We found OMV production to correlate with the recombinant production of a natural compound with versatile beneficial properties, the tripyrrole prodigiosin. Further, several P. putida genes were identified, whose up- or down-regulated expression allowed controlling OMV formation. Finally, genetically triggering vesiculation in production strains of the different alkaloids prodigiosin, violacein, and phenazine-1-carboxylic acid, as well as the carotenoid zeaxanthin, resulted in up to three-fold increased product yields. Consequently, our findings suggest that the construction of robust strains by genetic manipulation of OMV formation might be developed into a useful tool which may contribute to improving limited biotechnological applications.

This is an open access article under the terms of the Creative Commons Attribution-NonCommercial License, which permits use, distribution and reproduction in any medium, provided the original work is properly cited and is not used for commercial purposes.

© 2023 The Authors. *Microbial Biotechnology* published by Applied Microbiology International and John Wiley & Sons Ltd.

¹Institute of Molecular Enzyme Technology (IMET), Heinrich Heine University Düsseldorf, Düsseldorf, Germany

²Department of Environmental Biotechnology, Helmholtz Centre for Environmental Research (UFZ), Leipzig, Germany

³Institute of Biological Information Processing – Structural Biochemistry (IBI-7: Structural Biochemistry), Forschungszentrum Jülich, Jülich, Germany

⁴Ernst-Ruska Centre for Microscopy and Spectroscopy with Electrons (ER-C-3/Structural Biology), Forschungszentrum Jülich, Jülich, Germany

⁵Institute for Biological Information Processing 6 (IBI-6/ Structural Cellular Biology), Forschungszentrum Jülich, Jülich, Germany

⁶Department of Biology, Heinrich Heine University Düsseldorf, Düsseldorf, Germany

⁷Center for Biotechnology (CeBiTec), Bielefeld University, Bielefeld, Germany

⁸Bielefeld University, Medical School East Westphalia-Lippe, Bielefeld University, Bielefeld, Germany

⁹DWI-Leibniz-Institute for Interactive Materials, Aachen, Germany

¹⁰Functional and Interactive Polymers, Institute of Technical and Macromolecular Chemistry, RWTH Aachen University, Aachen, Germany

¹¹Institute of Bio- and Geosciences IBG-1: Biotechnology, Forschungszentrum Jülich, Jülich, Germany

INTRODUCTION

Secondary metabolites of microorganisms exhibit a variety of biological activities which make them applicable as pharmaceuticals, ingredients in cosmetics, and food additives. One approach to accessing these natural products is the biosynthesis in heterologous strains, which are engineered as whole-cell biocatalysts (Lin & Tao, 2017). In the last decades, *Pseudomonas* species have become promising bacterial cell factories for such bioproduction processes. One prominent representative of this group is *Pseudomonas putida*, mainly due to its inherent robustness as reviewed in detail in the last years (Bitzenhofer et al., 2021; Loeschcke & Thies, 2015, 2020; Nikel & de Lorenzo, 2018; Weimer et al., 2020).

The compounds which have been produced in $P.\ putida$ include toxic aromatic acids like p-coumarate or cinnamate (Calero et al., 2018; Molina-Santiago et al., 2016; Schwanemann et al., 2020), antimicrobial compounds like violaceins and phenazines (Askitosari et al., 2019; Domröse et al., 2017; Zhang et al., 2017), or prodiginines and glidobactins (Cook et al., 2021; Domröse et al., 2015; Loeschcke & Thies, 2020), as well as different terpenoids including zeaxanthin, β -carotene, and lycopene (Beuttler et al., 2011; Hernandez-Arranz et al., 2019; Sánchez-Pascuala et al., 2019).

Despite these success stories, the high-level production of natural compounds is still challenging, amongst other reasons, due to chemical stress caused by high product and substrate concentrations, respectively, which can damage biomolecules or membranes, ultimately compromising the bioprocess (Nicolaou et al., 2010). It is thus intriguing to understand how bacteria have naturally evolved different strategies to respond and adapt to chemical stress. In Pseudomonads, an active extrusion of a chemical stressor via efflux transporters to avoid its intracellular accumulation or damage recovery/prevention mechanisms (e.g., the use of chaperones or redox enzymes) are prominent strategies to deal with chemical stress (Bitzenhofer et al., 2021; Blanco et al., 2016; Bösl et al., 2006; Hartl et al., 2011; Henderson et al., 2021; Nicolaou et al., 2010; Roca et al., 2008). Further, Pseudomonas-characteristic and quite unique stress response is the conversion of cis- unsaturated fatty acids (FA) of the inner membrane (IM) to their trans-configuration by the cis-trans-isomerase (Cti) (Bitzenhofer et al., 2021; Heipieper et al., 2003; Tan et al., 2016). The Cti exerts an immediate response: The enzyme is described to be constitutively present in the periplasm and as soon as the membrane is sufficiently perturbed, it can access the cis-unsaturated FA in the membrane phospholipid bilayer and isomerises them to the corresponding trans-configuration (Mauger et al., 2021). Additionally, P. putida can also respond

by vesiculation to chemical stresses, i.e., releasing outer membrane vesicles (OMVs) into the extracellular space. This can be caused by structural changes in the cell envelope (Juodeikis & Carding, 2022). The two processes, cis-trans-isomerisation and OMV release, can be employed synchronously in response to the same stresses, but not obligatory so (Eberlein et al., 2018). The OMVs are mainly composed of phospholipids, lipopolysaccharides (LPS), and proteins (Avila-Calderón et al., 2021). Their release can lead to a more hydrophobic bacterial cell surface and thus enhance biofilm formation, which in turn increases bacterial resistance to chemical stressors (Atashgahi et al., 2018; Baumgarten et al., 2012). In addition, vesiculation can help to bring and/or keep the stressors out of the cell (Eberlein et al., 2019; Mozaheb & Mingeot-Leclercq, 2020) and OMVs may serve as an extracellular reservoir for chemical compounds, effectively reducing the concentration in or surrounding the cell (Domröse et al., 2015; Schwechheimer & Kuehn, 2015). An association of OMV release with natural bacterial export of secondary metabolites has been proposed (Batista et al., 2020; Choi et al., 2020; Mashburn & Whiteley, 2005; Tan et al., 2020). Recently, the engineering of such membrane structures was shown to enhance the recombinant production of hydrophobic metabolites in Escherichia coli (Yang et al., 2021).

To alleviate the difficulties of high-level microbial production, the construction of robust cell factories with specifically adapted tolerance features seems to be crucial. Here, we assess OMV formation as a biotechnologically exploitable tolerance trait. We present genetic engineering strategies to increase vesiculation and the production of different secondary metabolites in *Pseudomonas putida* KT2440.

EXPERIMENTAL PROCEDURE

Cultivation of P. putida

Pseudomonas putida wild-type KT2440 (Nelson et al., 2002) and the derived strains P. putida pig21, vio12, and PCA1 (Domröse et al., 2017), P. putida pigr11, -43, and -r44 (Domröse et al., 2019), as well as P. putida crt ΔX , which was constructed as previously described (Loeschcke et al., 2013; see Table S4), were cultivated under continuous shaking (130 rpm) at 30°C in 10 mL LB (lysogeny broth) medium (10 g L⁻¹ tryptone, 5 g L⁻¹ yeast extract, 10 g L⁻¹ sodium chloride; Carl Roth®). Antibiotics were added to the culture medium when appropriate to the following final concentrations: 25 μg mL⁻¹ kanamycin, 25 μg mL⁻¹ irgasan, 25 μg mL⁻¹ gentamicin, and 50 µg mL⁻¹ tetracycline. For chemical induction of OMV formation, P. putida KT2440 was exposed to 1 mM 1-octanol (Acros organics, part of Thermo Fisher Scientific), 50 μM PQS in DMSO

17517915, 2024. 1, Downloaded from https://ami-journals.onlinelibrary.wiley.com/doi/10.1111/1751-7915.14312 by Forschungszentrum Jülich GmbH Research Center, Wiley Online Library on [30/01/2024]. See the Terms and Conditions (https://onlinelibrary.wiley.com/terms

+and-conditions) on Wiley Online Library for rules of use; OA articles are governed by the applicable Creative Commons License

(Biomol GmbH), or 0.6 mM prodigiosin (in DMSO, final concentration 3%; for extraction and purification see Figure S15 and M5 in Appendix S1) after reaching the logarithmic growth phase. To induce gene expression or to manipulate gene expression, respectively, 10 mM L-arabinose was added.

Plasmid and strain construction

Oligonucleotides, plasmids, and strains, which were generated based on P. putida KT2440, are summarised in Tables S3 and S4.

All recombinant DNA techniques were essentially performed as described by Sambrook et al. (1989), using Escherichia coli strains DH5α (Hanahan, 1983) and Stellar™ cells (Takara Bio, Cat# 636763; see Table S4). Assembly procedures for vectors facilitating overexpression or repression of candidate genes are detailed in M1 in Appendix S1.

Plasmids were introduced into *P. putida* KT2440 by electroporation (Tu et al., 2016). Briefly, 1 mL of overnight cultures of P. putida strains was harvested by centrifugation (2 min, 11,000 g) and washed with 1 mL H₂O (MilliQ®) twice. The cells were resuspended in 80 μL H₂O (MilliQ®) and supplemented with 50 ng plasmid DNA. Electroporation was performed in a MicroPulser ($25\mu F$, 200Ω , 4.5-5 ms, $20 kV cm^{-1}$; Bio-Budget Technologies GmbH). Cells were incubated in 0.7 mL LB medium under continuous shaking (300 rpm) for 2h before plating on LB agar plates with an appropriate antibiotic.

Determination of cis-trans-isomerase (Cti) activity

Fatty acid extraction and methylation were adapted from previous studies (Bligh & Dyer, 1959; Morrison & Smith, 1964). Briefly, cell samples corresponding to an optical density (OD_{700nm}) of 1 in 1mL were harvested from P. putida cultures by centrifugation. Fatty acid methyl esters (FAME) were prepared by incubating the samples in 1 mL methanol and 1.75 mL chloroform under continuous shaking (1000 rpm) for 3 min. Then, 0.5 mL dH₂O was added, and the suspension was thoroughly mixed for 30s. Centrifugation (10 min, 1000 g) facilitated clear phase separation. Finally, the chloroform phase was transferred to a new glass vial (CS), and the solvent was removed by evaporation (Concentrator 5301; Eppendorf). For the methylation of fatty acids (FA), samples were incubated in BF3-methanol (Merck) for 15 min at 95°C (Morrison & Smith, 1964). Lastly, FAME were extracted with hexane and stored at 4°C. FAME analysis was performed using gas chromatography with a flame ionisation detector (GC-FID, 6890N Network GC System, 7683B Series

Injector; Agilent Technologies). The instrument used a CP-Sil 88 column (CP7488; Varian) in stationary phase and helium as carrier gas. The temperature program was 40°C, 2min isothermal, followed by a gradientincrease up to 220°C (8°C min⁻¹), and 10 min at 220°C. The FAME peak areas were used to determine their relative amounts. The FA was identified by co-injection of authentic reference compounds obtained from Supelco. Trans/cis ratio was calculated taking the sum of the FAME of cis-palmitoleic acid (C16:1Δ9cis) and cis-vaccenic acid (C18:1\Delta11cis) as divisor and the sum of their corresponding trans configuration as dividend (Heipieper et al., 1992).

Isolation of OMVs

Procedures were based on already published protocols by Heipieper and coworkers (Eberlein et al., 2019). After 7 h of cultivation (24 h for some experiments), P. putida cells were pelleted by centrifugation (at 5000 g and 4°C for 15 min) and to ensure that all cells were removed, the supernatant was filtered through a membrane with 0.45 μm pore size (Sarstedt). As we did not see any cells in either the TEM or the (MA)DLS analyses (see below), we consider the 0.45 µm-filter to be appropriate. For final isolation, OMVs were sedimented by ultracentrifugation (at 100,000 g and 4°C for 3h; rotor 50.2 Ti; Beckman Coulter). The obtained vesicle pellet was resuspended in 100 µL 10 mM HEPES buffer (pH 6.8) and used for characterisation. For TEM analysis, OMVs obtained from one isolation batch were further purified by ultracentrifugation using a density gradient (2%, 15%, 40%, and 50% glucose) at 100,000 g and 4°C for 18 h (rotor SW32 Ti; Beckman Coulter). OMV fractions were collected at sugar concentrations of approximately 10% and 30%, respectively (determined with a refractometer (OPTEC, Optimal Technology)). Vesicle bands at higher sugar concentrations (glucose concentration of about 40%-50%) were not collected due to accumulation of other impurities. Here, a larger batch of 50 mL LB medium was used, and the further procedure was applied unchanged.

OMV characterisation

Bradford assay

For an approximation of relative OMV quantity, the amount of proteins within the OMV fraction was determined by the Bradford assay as described before (Eberlein et al., 2019). For this purpose, 75 μL of a 10-fold (or 30-fold) OMV dilution (in 10 mM HEPES buffer, pH6.8) were mixed with 75 µL Bradford reagent (20 mg Coomassie Brilliant Blue G-250, 10 mL ethanol, 20 mL phosphoric acid, ad 200 mL) in a microtiter plate

17517915, 2024. 1, Downloaded from https://ami-journals.onlinelibrary.wiley.com/doi/10.1111/1751-7915.14312 by Forschungszentrum Jülich GmbH Research Center, Wiley Online Library on [30/01/2024]. See the Terms and Conditions

onditions) on Wiley Online Library for rules of use; OA articles are governed by the applicable Creative Commons License

(MTP), and the absorption was measured at 595 nm using a plate reader (Tecan) after 5 min of incubation. Bovine serum albumin (BSA) solutions were used for calibration (0 to 0.25 mg mL⁻¹). Notably, other large cellular surface structures like flagellar components that co-sediment with OMVs would influence the Bradford results (Bauman & Kuehn, 2006). For prodigiosincontaining OMVs, the Bradford readout was corrected to take the absorption of the red pigment into account (see Figure S1 and M2 in Appendix S1).

Nile red assay

The lipophilic fluorescent dye Nile red was used as an indicator preferentially staining membranes to analyse OMV fractions. In an MTP, 2 µL of a 2% solution of Nile red (in DMSO; Sigma-Aldrich) was mixed with a 10fold diluted OMV sample in a total volume of 150 μL. Fluorescence was measured using a plate reader (Tecan) with an excitation wavelength λ_{ex} = 543 nm, an emission wavelength $\lambda_{\rm em}$ of 598 nm, a bandwidth of 5nm, and a gain of 150.

Biofilm formation assay

Quantification of biofilm formation as an indirect measurement of surface hydrophobicity was conducted according to O'Toole (2011). Cells were cultivated in an MTP in presence of the stressor 1-octanol (1 mM) or inducer for manipulation of gene expression (10 mM Larabinose) at 30°C for 24 h. The supernatant was used to measure the optical density (OD_{580nm}) of the planktonic cells. For quantification, the wells were washed, dried, and supplemented with 150 µL of a 0.1% crystal violet (CV) solution. The MTP was incubated at room temperature for 10 min, washed and dried again. To solubilise the CV, 150 µL 40% acetic acid was used and the absorption of the samples was measured at 550 nm in a fresh MTP (diluted with H₂O) using a plate reader (Tecan).

To correct for differences in growth behaviour, the data of all direct or indirect OMV assays were normalised to the respective cell density at 580nm (or 700 nm in case of prodigiosin-containing samples).

DLS analysis

The average size of isolated OMVs was analysed by dynamic light scattering (DLS) using a SpectroSize 300 (Xtal Concepts) with a 660nm laser at a fixed angle. Isolated OMVs were diluted to a corresponding optical density $(OD_{580\,\mathrm{nm}})$ of 0.2. DLS does not allow straightforward determination of the exact amount of OMVs in a solution. However, the intensity of the scattered light

depends on the concentration, diameter, and refractive index of the scatterer in relation to the refractive index of the solution (Makra et al., 2015). As the OMV samples were isolated at the same cultivation time, processed identically and the OMVs had a similar size distribution, the measured intensity of the signal (i.e. count rate in kHz) can be indicative of the vesicle concentration. To test this correlation, the signal intensity of a vesicle sample diluted to different concentrations was determined by DLS and the dilutions were plotted against the signal intensity, which showed a linear correlation (see Figure S7). Hence, DLS data were evaluated as size distribution (diameter in nm) and signal strength (of the count rate in kHz).

For MADLS, a Zetasizer Ultra (Malvern Panalytical GmbH, Herrenberg, Germany) was used, operating at three different scattering angles ($\theta = 15^{\circ}$, 90° , 175°) and a temperature of 25°C. The isolated vesicle fractions (after 7 or 24h) were diluted 10-fold in HEPES buffer (10 mM, pH6.8) for measurements in triplicates and analysed using a DTS0012 cuvette. The software ZSxplorer was used to analyse the results.

TEM analysis

For imaging, isolated OMV samples (3 µL) were added to a glow-discharged Formvar-carbon film, hexagonal, 300-mesh copper grid, washed two times with H₂O (MilliQ®; 15s) and stained with 2% uranyl acetate solution for 30 s. Surplus uranyl acetate was removed with a filter paper. Prepared grids were analysed using a TALOS L120C G2 transmission electron microscope (ThermoFisher Scientific) operated at 120 keV. Images were taken using the TEM Imaging & Analysis software (TIA; Thermo Fisher Scientific) on a 4k×4k Ceta M16 CEMOS camera.

Transcriptome analysis

For transcriptome analysis, cells were cultivated as described above, the cell pellet was harvested after 7h, adjusted to an optical density (OD_{700 nm}) of 1 and flash frozen.

Total RNA was isolated from three biological replicates using Quick-RNA Miniprep Plus kit (Zymo Research). The samples were treated with DNAse (Zymo Research), and RNA was again purified with an RNA Clean&Concentrator-5 kit (Zymo Research). Ribosomal rRNA was removed with a riboPOOL for bacteria (siTOOLs Biotech GmbH). The purity of RNA and removal of rRNA was tested with an Agilent RNA Pico 6000 kit and an Agilent 2100 Bioanalyzer (Agilent Technologies). TruSeq Stranded mRNA Sample Preparation guide (Illumina) was then used to construct the cDNA library. The constructed cDNA library was

17517915, 2024, 1, Downloaded from https://ami-journal

online library. wiley.com/doi/10.1111/1751-7915.14312 by Forschungszentrum Jülich GmbH Research Center, Wiley Online Library on [30/01/2024]. See the Terms and Conditions (https://onlinelibrary.wiley.

and-conditions) on Wiley Online Library for rules of use; OA articles are governed by the applicable Creative Commons License

then sequenced with Illumina NextSeq500 high output mode paired-end using a read length of 75 bases.

Transcriptomics sequencing raw data files are available at the ArrayExpress database (www.ebi.ac.uk/ arrayexpress) under accession no. E-MTAB-12470.

The paired-end cDNA reads were mapped to the P. putida KT2440 genome sequence (accession number AE015451.2; Belda et al., 2016; Nelson et al., 2002) using bowtie2 v2.2.7 (Langmead & Salzberg, 2012) with default settings for paired-end read mapping. All mapped sequence data were converted from SAM to BAM format with SAMtools v1.3 (Li et al., 2009) and imported to the software ReadXplorer v.2.2 (Hilker et al., 2016). Differential gene expression analysis of three biological replicates was performed using DESeq2 (Love et al., 2014) with ReadXplorer v2.2 (Hilker et al., 2016).

For significance of differentially transcribed genes, we used an adjusted p-value cutoff of ≤0.01 and a signal intensity ratio (M-value) cutoff of ≥ 2 or ≤ -2 .

Natural compound production in *P.* putida KT2440

Pseudomonas putida KT2440-derived previously generated strains, which carried the different biosynthetic gene clusters in the genome under a constitutive promoter (see Table S4), were transformed with plasmids for manipulation of the expression of candidate genes by electroporation. The cells were cultivated in 1 mL LB medium and incubated overnight in FlowerPlates® (Beckman Coulter GmbH (formerly m2p-labs GmbH)) at 30°C and shaking at 1200 rpm in a ThermoMixer® C (Eppendorf AG). For P. putida PCA1, Round Well Plates (Beckman Coulter GmbH (formerly m2p-labs GmbH)) were used instead of FlowerPlates® to lower oxygen transfer rates (culture volume: 750 µL). Main cultures were inoculated to an optical density (OD_{700nm}) of 0.05 in LB medium already containing 10 mM L-arabinose as inducer for gene overexpression or for the implementation of the CRISPRi system. The cells were incubated under above-described conditions for 48 h.

Extraction of natural products

Samples from cultivation of the producers were fractionated into cell pellet and supernatant by centrifugation (at 15,000 g and 4°C for 5 min). The pellets were extracted with 1 mL ethanol (p.a.; for prodigiosin: acidified ethanol (4% 1 M HCl) was used). The extracts were cleared by centrifugation (15,000 g, 10 min). Additionally, compounds were extracted from the supernatant by two-phase-extraction with ethyl acetate (2×500 μL; for PCA, the supernatant was acidified with 100 μL 6 M HCI) and evaporated afterwards (Concentrator 5301;

Eppendorf). After evaporation, products (except of PCA samples) were dissolved in 150 µL ethanol (p.a.; for prodigiosin, acidified ethanol was used). As PCA mainly accumulates in the supernatant, extracts from the supernatant were dissolved in 1 mL ethanol (p.a.) after evaporation.

Determination of product titres and analytics

Prodigiosin, (deoxy) violacein, and zeax anthin were quantified spectrophotometrically based on their molar extinction coefficients (prodigiosin: $\varepsilon_{535\,\mathrm{nm}} = 139,800\,\mathrm{M}^{-1}\,\mathrm{cm}^{-1}$; (deoxy)violacein: $\varepsilon_{575\,\mathrm{nm}} = 25,400\,\mathrm{M}^{-1}\,\mathrm{cm}^{-1}$; zeaxanthin: $\varepsilon_{450\,\mathrm{nm}} = 144,500\,\mathrm{M}^{-1}\,\mathrm{cm}^{-1}$ (Domröse et al., 2015; Loeschcke et al., 2013; Rodrigues et al., 2012)) in acidified (prodigiosin) or pure (zeaxanthin, (deoxy)violacein) ethanol, respectively, using a plate reader (Tecan, Maennedorf, Switzerland).

Phenazine-1-carboxylic acid (PCA) was quantified via HPLC-PDA analysis using an LC-10Ai series (Shimadzu GmbH), equipped with an SPD-M10Avp photodiode array detector (PDA). The column oven temperature and the flow rate were set to 30°C and 1 mL min⁻¹. As mobile phase water (A) and acetonitrile (B), both supplemented with 0.1% formic acid, were used. A C30-reverse-phase HPLC column (250 × 4.6 mm, 5 mm particle size, YMC-Europe GmbH) was applied and 10 µL of extracted samples were injected onto the column. Analyses started at 5% B for 2.5 min, before a gradient was used for 16.5 min to reach 98% B. This ratio was maintained for 2min and then decreased again to 5% B within 1min. For reequilibration, the last condition was again maintained for 5 min (Domröse et al., 2017). Chromatograms were recorded at 366 nm. To identify and quantify the PCA signal, a reference (Apollo Scientific) was used for calibration (0-400 mg L⁻¹). PCA signals were observed at a retention time of 18.1 min.

RESULTS AND DISCUSSION

OMV release is a natural response of P. putida KT2440 to chemical stress

To identify a tolerance trait that might provide a useful starting point for the engineering of robust production chassis strains, the native stress response of P. putida KT2440 were examined first. We chose to focus on the characteristic membrane adaptation responses of *Pseudomonas* species to environmental stress (i.e., Cti activity and vesiculation), especially triggered by hydrophobic compounds. The established method to assess the activity of Cti relies on the determination of the ratio of trans- to cis-unsaturated membrane FAs

the prodigiosin biosynthetic *pig* gene cluster (Domröse et al., 2017).

Cell samples were subjected to analyses regarding changes in the *trans/cis* ratio of unsaturated membrane FA. In addition, vesicle fractions were isolated from the supernatant (see Figure 1A) and their protein content was determined as an estimation of produced vesicles. The untreated wild type was used as reference for the

via GC-MS using common protocols for extraction and derivatisation (Heipieper et al., 1995). One common method to indirectly detect OMV formation is the quantification of proteins in the vesicle fraction which can be obtained by ultracentrifugation of culture supernatants (Eberlein et al., 2019). Positive controls for both assays were derived from previous studies: P. putida KT2440 wild type was treated with 1-octanol, which is known to trigger both Cti activity and vesiculation (Baumgarten et al., 2012; Eberlein et al., 2018, 2019; Heipieper et al., 1995), and with the Pseudomonas quinolone signal (PQS), a quorum sensing-associated compound that is known to induce vesiculation (Mashburn-Warren et al., 2009). In addition, we analysed the effect of the hydrophobic antimicrobial tripyrrole prodigiosin on the cell envelope stress response since P. putida KT2440 has been shown to be especially suitable for the production of this compound (Domröse et al., 2015, 2019). For this, we tested the effects of both, the external addition of prodigiosin to the wild type bacteria and the intrinsic prodigiosin production by P. putida pig21, which was previously established by chromosomal integration of

evaluation of all other samples (see Figure 1B,C).

As expected for the positive control, 1-octanol triggered both Cti activity and vesiculation. Interestingly, PQS only caused vesicle formation but no change in the *trans/cis* ratio of FA, while prodigiosin treatment caused the opposite response. External addition of prodigiosin resulted in a significant increase in Cti activity but did not induce hypervesiculation. The production strain *P. putida* pig21, like the PQS-treated wild type, showed again no Cti response but strong vesiculation. Interestingly, the isolated vesicle fraction of this strain exhibited the characteristic bright red colour of prodigiosin, suggesting that the compound had accumulated in these structures (see Figure 1A).

17517915, 2024, 1, Downloaded from https://ami-journals.onlinelibrary.wiley.com/doi/10.1111/1751-7915.14312 by Forschungszentrum Jülich GmbH Research Center, Wiley Online Library on [30:01/2024.] See the Terms

and-conditions) on Wiley Online Library for rules of use; OA articles are governed by the applicable Creative Commons License

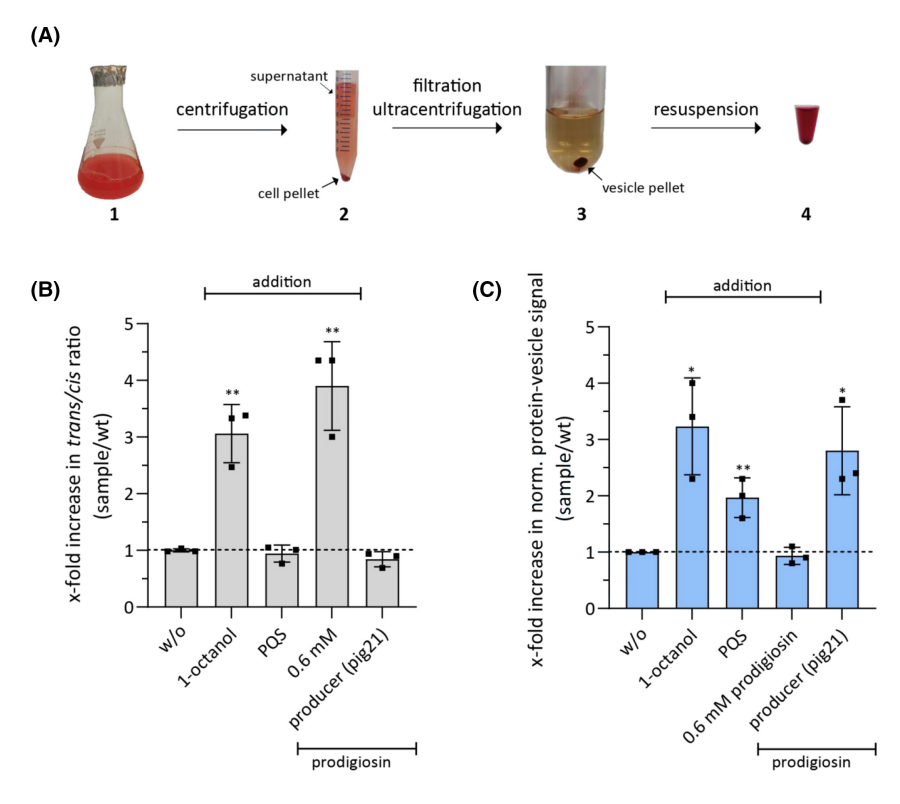


FIGURE 1 Cell envelope stress response of *Pseudomonas putida* after treatment with different stressors. (A) Procedure of OMV isolation using the prodigiosin producing strain P. putida pig21 as an example. Starting from a production culture (step 1), cells were harvested (step 2) and the supernatant was filtered (0.45 μ m pore size). Vesicle isolation was performed by ultracentrifugation (step 3). Subsequently, the obtained vesicle pellet was resuspended in buffer (step 4). (B) Increase in trans/cis ratio of membrane FA (indicative of Cti activity) of different P. putida samples. (C) Increase in protein-vesicle signal calculated from Bradford assay of different P. putida samples (correction for prodigiosin-containing samples had to be applied (see Figure S1)). The samples are taken after 7h of cultivation (logarithmic phase) and the data are normalised to the cell density of the cell culture. Data are shown as x-fold increase of values of treated P. putida KT2440 wild type cells (1 mM 1-octanol, 50 μ M PQS or 0.6 mM prodigiosin) or the prodigiosin producer strain P. putida pig21 compared with the wild type sample without any treatment (w/o; indicated by the dashed line). The data are mean values of independent triplicate measurements with their respective standard deviation. Significant differences in comparison to the untreated wild type (w/o) are indicated by asterisks (determined by T-test; * $p \le 0.05$, ** $p \le 0.01$).

Hence, we find that the tested compounds, which share a relatively high value for the partition coefficient logP(1-octanol=3.0; PQS=4.74; prodigiosin=4.07 (calculated using XLOGP3 software (Cheng et al., 2007))) cause a membrane stress response. Interestingly, the quality of membrane adaptation clearly depends on the type of chemical stress. Further, the membrane adaptations appear to be influenced by the compound location and concentration dynamics ("shock treatment" of prodigiosin applied externally as a single full dose application versus steady increase of internally produced compound over the time of cultivation). External "shock treatment" might perturb the membrane to cause fatty acid conversion by Cti, while the production might be accompanied by the general vesiculation stress response which prevents Cti-critical concentrations at the IM. However, the validation of such hypotheses will require further analyses since any potential dynamic responses were not resolved in the end point measurements of the present study. Importantly, our data indicate that the meaningfulness of results obtained from examining cell responses after external application of a chemical stressor as a proxy for a production scenario can be limited and it is useful to analyse production strains themselves.

The observation of enhanced vesiculation in a P. putida production strain prompted us to investigate the OMV formation in this context in more detail. The quantification of OMVs by Bradford-based protein quantification as applied here is widely established (Eberlein et al., 2019; Rodriguez & Kuehn, 2020; Roier et al., 2016). However, potential changes in the protein content of OMVs in response to different conditions may influence the results (Bitto et al., 2021). Hence, the vesicle fraction of strain pig21 was additionally subjected to particle analysis by multi angle dynamic light scattering (MADLS), which validated enhanced vesicle formation in comparison to the wild type (see Table S1). We further characterised the OMVs produced by P. putida pig21 in comparison to the OMV-triggering controls by fixed angle dynamic light scattering (DLS) and transmission electron microscopy (TEM; see Figure 2). The OMV diameters determined by DLS ranged between 135 and 170 nm (comparable to the MADLS results), which is in the same range as previously described for *P. putida* OMVs (Baumgarten et al., 2012; Roier et al., 2016). Further, qualitative TEM analyses revealed that both OMVs from PQS-treated cells and P. putida pig21 producer cells apparently formed clustered agglomerates.

The formation of OMVs thus appears to be a native response of *P. putida* KT2440 to the production of the bioactive compound prodigiosin. We next evaluated whether vesiculation and compound production are quantitatively correlated. To this end, three previously established *P. putida* strains, pig-r43, pig-r11, and pig-r44, which produce prodigiosin at different levels

(Domröse et al., 2019), were subjected to OMV characterisation. Here, low, moderate, and strong OMV formation were found to correlate with the low, moderate, and high-level prodigiosin titres of the respective strains (see Figure 3A).

Additionally, the effect of OMV release triggered by chemical treatment with PQS and 1-octanol on the prodigiosin production levels of *P. putida* pig21 was investigated. Here, we also observed a correlation between OMV formation and compound production (see Figure 3B). An effect of the chemical stress on the *pig* gene transcription levels was excluded via RT-qPCR (see Figure S3). Hence, we deduced that the process of vesicle release itself may positively influence prodigiosin production titres and, therefore, both processes appear to influence each other: An increase in the amount of intracellularly produced prodigiosin increases the formation of OMVs and vice versa.

By measuring product concentration in the different fractions (pellet and OMV fraction; Figure 3), we demonstrate prodigiosin accumulation not only in the pellet but also in the vesicles. This confirms our initial visual observation (see Figure 1A). It is also consistent with the compound's hydrophobicity, based on which it was expected that prodigiosin would interact with the OMVs rather than accumulate in the aqueous medium.

Vesiculation can be triggered by genetic manipulation of *P. putida*

As a next step, we aimed to identify candidate genes associated with vesiculation that might allow targeted genetic manipulation of the process.

We first approached this question in an attempt to uncover the specific adaptations in vesiculating strains based on the above-described observations. To this end, we analysed transcriptomic data of the prodigiosin producing strain P. putida pig21 in comparison to the wild type strain and the wild type triggered to form OMVs by addition of PQS or 1-octanol. Interestingly, both prodigiosin production and 1-octanol addition caused higher changes in the overall number of up- or down-regulated genes than PQS addition (see Table 1, see also Figure S4). This observation, along with the finding that PQS treatment did not increase Cti activity, is consistent with the fact that PQS cannot readily cross the outer membrane (OM) (Florez et al., 2017). Among the sample sets of strain pig21 and 1-octanol-treated wild type cells, we identified six common genes, which were highly up- or down-regulated compared to the untreated wild type (PP_2805 (ethA), PP_2807, PP_3494, PP_3533, PP_0710, and PP_4524; see Figure 4), which were thus selected as candidate genes presumably associated with OMV formation.

Interestingly, we detected the Cti transcript in all of the samples in comparable copies. It was thus not

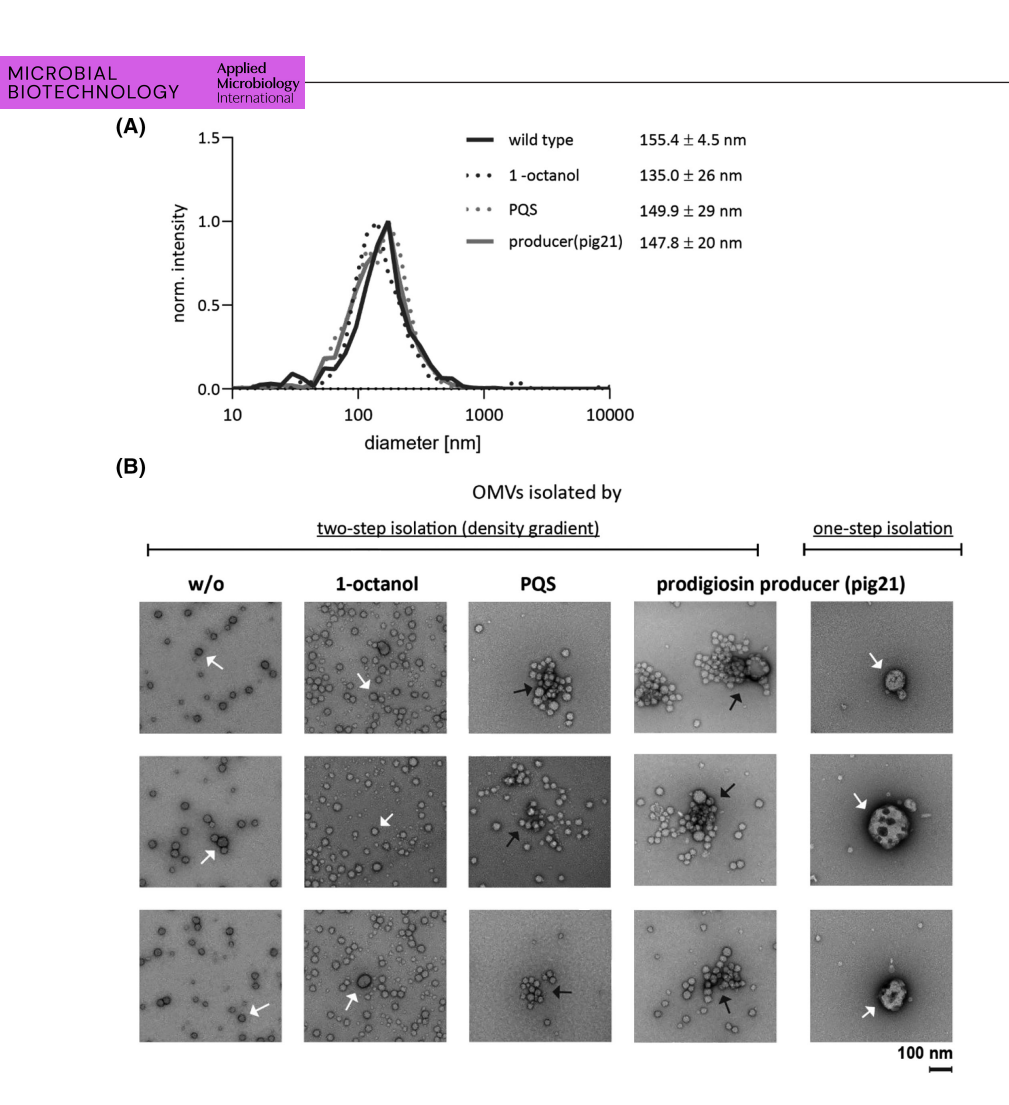


FIGURE 2 Pseudomonas putida wild type and prodigiosin producer strain OMVs. (A) Diameter of isolated OMVs of differently treated *P. putida* KT2440 wild type samples (1 mM 1-octanol or 50 μM PQS; w/o: without addition of a stressor) and the prodigiosin producer strain *P. putida* pig21 determined by DLS measurements (diameter plot: intensity is normalised to maximum). Here, OMVs were isolated by a single ultracentrifugation step (one-step isolation). (B) TEM analysis of negatively stained OMVs of the above measured samples. Left side: for higher background purity, the OMV samples were additionally purified using a glucose density gradient (2%–50%) after the first ultracentrifugation step (two-step isolation). Here, only smaller types of vesicles were collected (20–90 nm). Right side: vesicles from the producer *P. putida* pig21 are shown after one-step isolation (identical to DLS sample preparation). Vesicles showed diameters of about ~143.9±45 nm, comparable to the results from DLS measurements (see A and Table S1). White arrows indicate vesicles, black arrows clustered agglomerates. For every OMV sample, TEM images of three different grid squares are shown (see also Figure S2). Magnification: 92,000×. Scale: 100 nm.

regulated, although 1-octanol treatment was shown to enhance the *trans/cis* ratio of unsaturated membrane FA. This is in accordance with previous descriptions of the enzyme being constitutively expressed and constantly present in the periplasm, from where it can slide into a perturbed membrane to reduce fluidity and increase cell stability (Eberlein et al., 2018; Mauger et al., 2021).

As a second approach, additional candidate genes were identified based on existing knowledge. The release of OMVs can be caused by (i) a reduction of local connections between the OM and the peptidoglycan layer (PG), (ii) an increase in local OM curvature, or (iii) an increase in periplasmic pressure (Juodeikis & Carding, 2022). We looked for different genetic targets whose native function is connected to one of the potential

OMV generation mechanisms and whose manipulation can thus affect vesiculation. Several genes have been identified as putative candidates involved in OMV formation in Gram-negative bacteria (see Table S2; Avila-Calderón et al., 2021; Juodeikis & Carding, 2022; Kulp & Kuehn, 2010; Schwechheimer & Kuehn, 2015). While P. putida features similar genes or respective proteins, which could be identified by sequence homology searches (see M6 in Appendix S1), their role in OMV formation has never been described or examined. Based on the results of the literature- and sequencebased searches as well as transcriptome analysis, we selected a set of 21 candidate genes potentially associated with vesiculation, which encode inner and outer membrane proteins (IMPs and OMPs), regulatory elements, periplasmic proteins, PG-degrading enzymes,

17517915, 2024, 1, Downloaded from https://ami-journals.onlinelibrary.wiley.com/doi/10.1111/1751-7915.14312 by Forschungszentrum Jülich GmbH Research Center, Wiley Online Library on [30/01/2024]. See the Terms and Conditions

and-conditions) on Wiley Online Library for rules of use; OA articles are governed by the applicable Creative Commons License

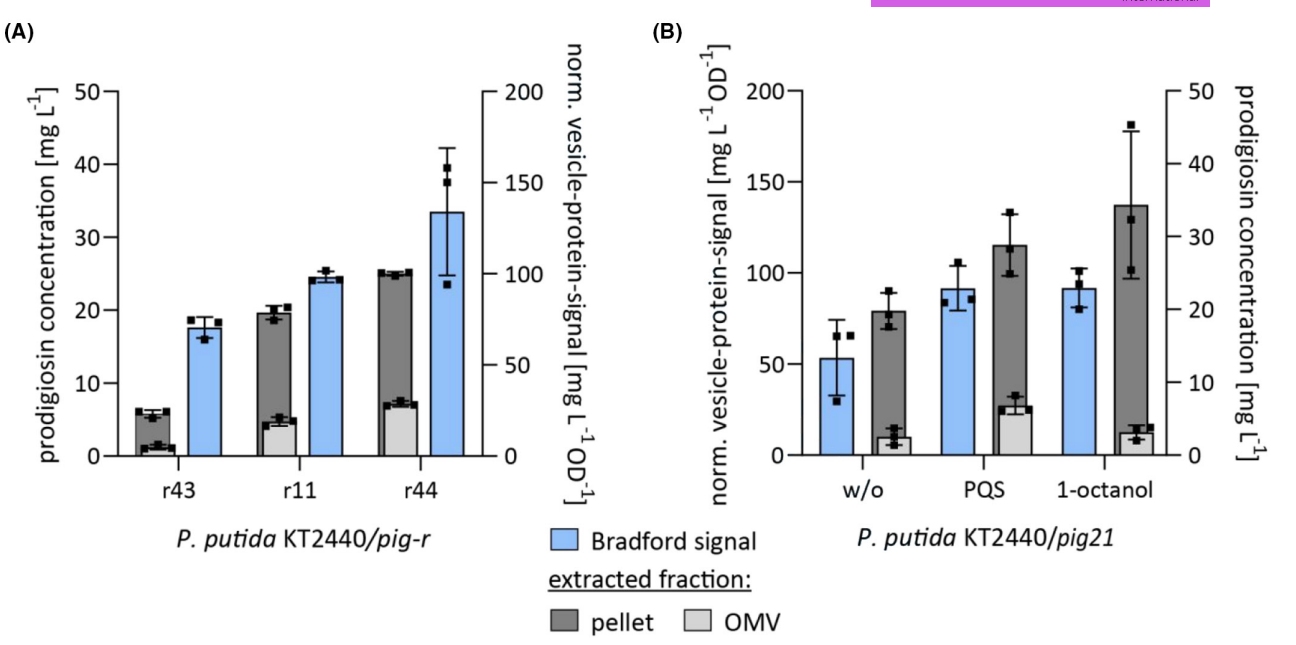


FIGURE 3 Correlation between prodigiosin production and OMV formation in P. putida producer strains. (A) Investigation of the effect of prodigiosin production (grey) on vesicle formation (blue) using a low (pig-r43), a moderate (pig-r11), and a high (pig-r44) prodigiosin producer strain. (B) Investigation of the effect of OMV formation (blue) on the prodigiosin titres (grey) of the producer strain P. putida pig21. For this, vesiculation is triggered by addition of different vesiculation-inducing stressors (1 mM 1-octanol or 50 μM PQS; w/o: without addition of a stressor). OMV amount was analysed by Bradford assay (correction for prodigiosin containing samples had to be applied (see Figure S1)). The prodigiosin concentration was determined in both fractions, the pellet fraction (dark grey) and the isolated OMV fraction (light grey). All samples were taken after 24 h of cultivation, and the data are normalised to the cell density of the cell culture. The data are mean values of independent triplicate measurements with their respective standard deviation. Bars are sorted in ascending order.

TABLE 1 Overall number of up- or down-regulated genes (identified by transcriptome analysis).

Number of regulated genes ^a Up Down	Pseudomonas Putida KT2440									
	Strain pig21	Wild type + 1-octanol	Wild type + PQS							
Up	53	29	2							
Down	74	7	_							

^aFor significance of differentially transcribed genes as compared to the untreated wild type, we used an adjusted p-value cutoff of ≤0.01 and a signal intensity ratio (M-value) cutoff of ≥2 or ≤-2.

or enzymes involved in iron homeostasis (see Table 2). For each gene, a manipulation strategy to either up- or down-regulate the expression was chosen, depending on the previous findings.

Thus far, knockout strains have been generated and described in the literature for many of the chosen targets. To conveniently test a range of candidate genes in the present study, we chose to implement repression of the target gene expression (i.e., respective protein production) by CRISPR interference (CRISPRi; Batianis et al., 2020; Qi et al., 2013; Tan et al., 2018). With this method, the repression is 'portable on a plasmid' and can be easily implemented and tested in several strain backgrounds, as has been done before to manipulate

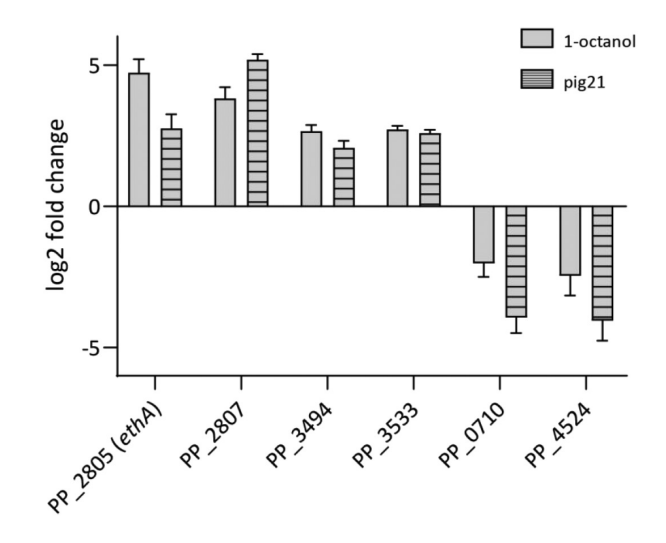


FIGURE 4 Transcriptome analysis of differently stressed Pseudomonas putida cells. Highly up- or down-regulated genes of 1-octanol treated P. putida KT2440 and P. putida pig21 cells as compared to the untreated wild type. Filled bars show M-values for 1-octanol-treated cells, hatched bars the prodigiosin producer. The data are mean values of independent triplicate measurements with their respective standard deviation.

OMVs (Yu et al., 2023). We further regarded repression advantageous over complete deletion since it should also allow addressing rather essential genes.

1751/7151, 2024, 1, Downloaded from https://aini-journals.onlinelibrary.wiley.com/doi/10.1111/751-7151.14312 by Forschangeszentrum Julich GmbH Research Center, Wiley Online Library for rules of use; OA articles are governed by the applicable Creative Commons License

Candidate genes that may affect OMV formation by Pseudomonas putida KT2440 (sorted by localisation). TABLE 2

18	3	MICRO BIOTEC	BIAL CHNOL	OGY	Applied Microbi Internat	Applied BITZENHOFER International												ET A	.L.				
Manipulation strategy (regulation)		Down-regulation (CRISPRi, NT strand)	Down-regulation (CRISPRi, T strand)	Down-regulation (CRISPRi, NT strand)	Up-regulation (overexpression)		Up-regulation (overexpression)	Down-regulation (CRISPRi, NT)	Down-regulation (CRISPRi, NT strand)		Down-regulation (CRISPRi, NT strand)	Up-regulation (overexpression)	Down-regulation (CRISPRi, NT strand)	Down-regulation (CRISPRi, NT strand)		Up-regulation (overexpression)	Down-regulation (CRISPRi, NT strand)	Down-regulation (CRISPRi, NT strand)	Up-regulation (overexpression)	Up-regulation (overexpression)		Down-regulation (CRISPRi, NT strand)	Up-regulation (overexpression)
Identification strategy		Literature, sequence (BLASTp)	Literature, sequence (BLASTp)	Literature, sequence (BLASTp)	Literature, sequence (BLASTp)		Literature, sequence (BLASTp)	Literature, sequence (BLASTp)	Literature, sequence (BLASTp)		Literature, sequence (BLASTp)	Literature, sequence (BLASTp)	Literature, sequence (BLASTp)	Literature, sequence (BLASTp)		Literature, sequence (BLASTp)	Literature, sequence (BLASTp)	Literature, sequence (BLASTp)	Transcriptomics	Transcriptomics	. ;	Transcriptomics	Transcriptomics
Product description (Pseudomonas genome DB; Winsor et al., 2016)		OM lipoprotein	Peptidoglycan-associated lipoprotein	OmpA family OM protein	Outer membrane-bound lytic murein transglycolase A		NLP/P60 family protein	Penicillin-insensitive transglycosylase/ penicillin-sensitive transpeptidase	Acyl-homoserine lactone acylase		Phospholipid ABC transporter permease	Hypothetical protein	Glycosyl transferase	Colicin S4/filamentous phage transport protein		RNA polymerase sigma E factor	Bifunctional heptose 7-phosphate kinase/heptose 1-phosphate adenylyltransferase	ADP-heptose-LPS heptosyltransferase	FAD-containing monooxygenase	Hypothetical protein		Hypothetical protein	Hypothetical protein
Locus tag (Pseudomonas genome DB; Winsor et al., 2016)		PP_2322	PP_1223	PP_1087	PP_4971		PP_1669	PP_5084	PP_2901		PP_0959	PP_0287	PP_1804	PP_1221		PP_1427	PP_4934	PP_0342	PP_2805	PP_2807		PP_0710	PP_3494
Pseudomonas putida protein [Genbank ID]	Outer membrane (OM)	Oprl (Lpp) [NP_744471]	OprL (Pal) [NP_743383]	OmpA [NP_743248]	MItA [NP_747074]	Periplasm (PP)	Spr [NP_743826]	MrcA [NP_747185]	PvdQ [NP_745045]	Inner membrane (IM)	MIaE [NP_743120]	PP_0287 (AsmA) [NP_742454]	WbpL [NP_743959]	TolA [NP_743381]	Cytoplasm (CP)	RpoE [NP_743585]	HIdE [NP_4934]	WaaC [NP_742509]	EthA [NP_744949]	PP_2807 [NP_744951]	Unknown localisation	PP_0710 [NP_742871]	PP_3494 [NP_745631]

17517915, 2024. 1, Downloaded from https://ami-journals.onlinelibrary.wiley.com/doi/10.1111/1751-7915.14312 by Forschungszentrum Jülich GmbH Research Center, Wiley Online Library on [30/01/2024]. See the Terms and Conditions (https://onlinelibrary.wiley. conditions) on Wiley Online Library for rules of use; OA articles are governed by the applicable Creative Commons License

Therefore, we assembled a broad-host-range CRISPRi vector (pBTBX-2-CRISPRi, see Figure S5A) based on a catalytically inactive variant of the endonuclease Cas9 from Streptococcus pyogenes (SpCas9 D10A H840A). We first evaluated the effect of the newly constructed system on both prodigiosin and pyoverdine production. Here, we could verify the functionality of the CRISPRi system in dependence on the guidingRNA (gRNA) target DNA strand (template (T) or non-template (NT)), on the distance from the translational start codon, as well as on the concentration of the inducer L-arabinose (see Figure S5B). Due to the most effective downregulation, gRNAs targeted to the NT DNA strand close to the translational start codon were selected for down-regulation of the expression of candidate genes. However, the efficiency of down-regulation was dependent on the addressed gene (see Figure S5B). Accepting the limitation that gene-to-gene differences in down-regulation efficiency may occur, we deemed the system applicable to conveniently screen the candidate genes, for which respective gRNA-encoding sequences were cloned.

Candidate genes, whose up-regulation appeared promising, were cloned in the vector pBTBX-2-mcs (Prior et al., 2010), which facilitates L-arabinose-dependent expression (see Figure S6; Hogenkamp et al., 2022). Using both strategies, plasmids for the manipulation of 18 targets could be cloned (for *tonB*, PP_3533, and PP_4524, which were also regarded as promising, cloning was not successful) and introduced into *P. putida* KT2440 to test whether a hypervesiculation phenotype could be implemented.

It is unknow which aspect of vesiculation in terms of quality and quantity might be relevant for supportive effects of natural compound production. Hence, we performed different assays: Bradford and Nile red assay were applied for protein- or lipid-quantification in isolated vesicle fractions as these are also the commonly addressed components for quantifying OMV yields (Klimentová & Stulík, 2015). Further, we analysed the particles via DLS to investigate vesicle sizes; moreover, as the DLS signal intensity may be correlated to the scatterer concentration (see Figure S7), the signal strength was evaluated as potential indicator of relative OMV concentrations. In addition, we measured biofilm formation using crystal violet (CV; Baumgarten et al., 2012; Kulp & Kuehn, 2010) as a measure for vesiculation-induced, increased cell surface hydrophobicity and aggregation (see Figure 5). For all assays, 1-octanol treatment was again used as a positive control. To exclude any effect by dcas9 expression on the vesiculation response, a CRIPSRi empty vector control (ev (Ci)) was used in all assays.

The different assays for analysis of vesiculation gave comparable results for down- or up-regulated expression of most target genes. Since OMV features may well change upon manipulations, we did not expect to find the exact same outcome in all assays for all strains. Around a third of the manipulations had no or only a minor impact. Notably, in the cases where manipulation relied on CRISPRi, the screening approach cannot distinguish between a manipulation having no effect and a guide RNA failing to implement repression of target gene expression. Around two thirds of the manipulations gave moderately to significantly increased signals. Interestingly, manipulation of OMPs barely caused a change in vesiculation in samples taken from the logarithmic growth phase, however, a stronger effect became apparent after 24h (see also Figure S8). We also observed differences in the vesiculation phenotype of bacteria examined during the logarithmic and stationary growth phases e.g., upon overexpression of sigma factor rpoE, which regulates cell envelope integrity (Rouvière et al., 1995; Schwechheimer et al., 2013). In contrast, the sizes of vesicles produced by differently engineered hypervesiculating strains did not vary significantly (see Figure 5D and Figure S9). In summary, we could identify a range of genes, whose manipulation led to the implementation of hypervesiculation phenotypes in P. putida KT2440.

For validation, we aimed to delete the two CRISPRidownregulated genes, pvdQ and hldE. However, hldE could not be deleted despite several attempts. This underlines the usefulness of a CRISPRi-based downregulation of genes of interest. The pvdQ mutant, which was obtained without difficulties, showed a similarly increased protein and lipid signal in the vesicle fraction as the respective CRISPRi strain (see Figure S10). A limited number of manipulations were chosen for an assessment of tolerance engineering in the generation of robust chassis for natural compound production. We selected the target genes PP_2087 (up), ethA (up), hldE (down), mltA (up), and pvdQ (down) because their manipulation led to effects across all assays, which was achieved by both, up- and downregulation approaches. Moreover, these included different types of proteins with different cellular localisations, which are associated with different vesiculation mechanisms.

PP_0287 encodes a protein with sequencesimilarity to E. coli AsmA, which is predicted to be localised at the IM and to play a role in the assembly of OMPs, LPS biogenesis, OM fluidity, and the tolerance towards hydrophobic antibiotics (Deng & Misra, 1996; Levine, 2019; Misra & Miao, 1995; Xiong et al., 1996). EthA is a cytoplasmatic FAD-containing monooxygenase exhibiting the consensus motifs of Baeyer-Villiger monooxygenases, which was upregulated in both, 1-octanol-treated and prodigiosinproducing cells and might naturally be involved in the degradation of alkanes and other xenobiotics (Blum et al., 2021; Minerdi et al., 2012; Rehdorf et al., 2007; Van Bogaert et al., 2011; Winsor et al., 2016). However, the association of this monooxygenase with cell envelope properties and vesiculation is unclear.

17517915, 2024, 1, Downloaded from https://ami-journals.onlinelibrary.wiley.com/doi/10.1111/1751-7915.14312 by Forschungszentrum Jülich GmbH Research Center, Wiley Online Library on [30/01/2024]. See the Terms

and Conditions (https://onlinelibrary.wiley.com/terms-and-conditions) on Wiley Online Library for rules of use; OA articles are governed by the applicable Creative Commons License

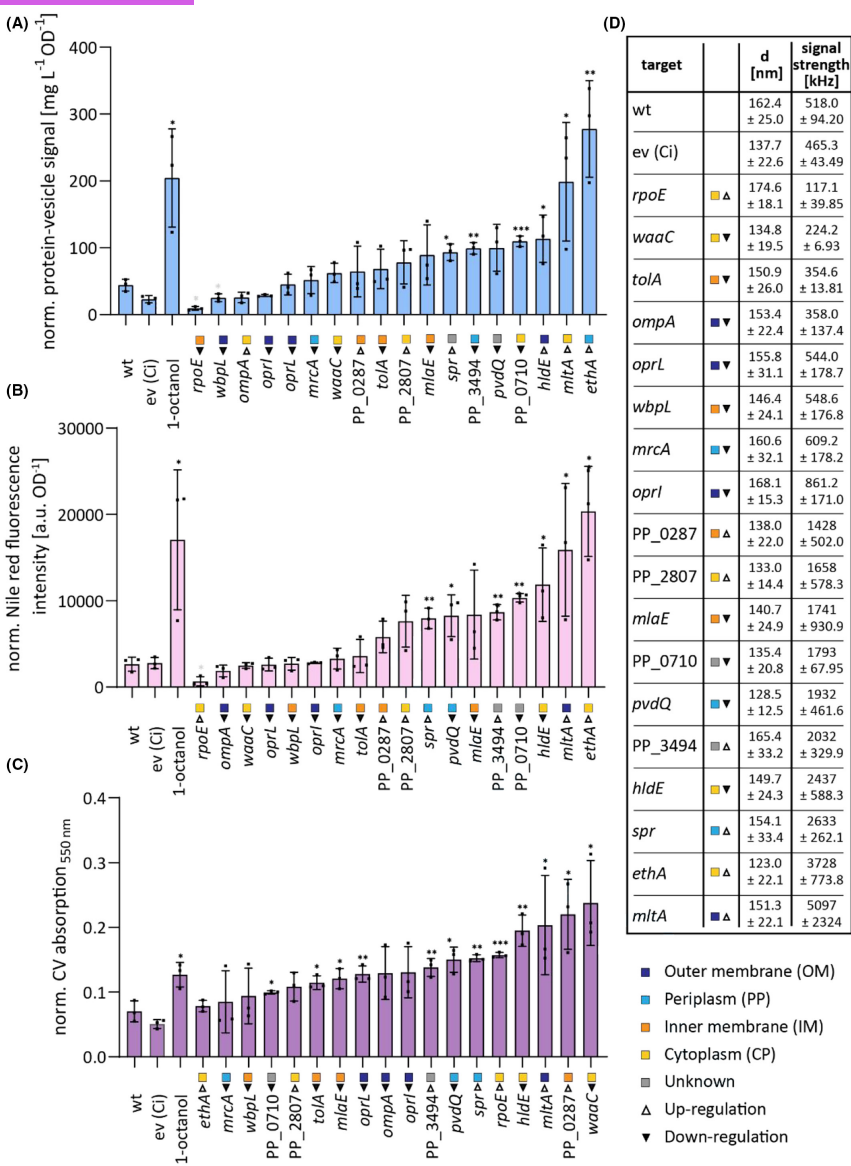


FIGURE 5 Characterisation of OMVs formed by engineered $Pseudomonas\ putida$ strains. (A) Amount of protein in the OMV fraction isolated from engineered $P.\ putida$ strains calculated by Bradford assay (based on $\lambda_{max} = 595\,\text{nm}$) after growth for 7 h (logarithmic phase). The data are normalised to the cell density of the cell culture. (B) Amount of lipid in the OMV fraction formed by engineered $P.\ putida$ strains calculated by Nile red assay (based on $\lambda_{ex} = 543\,\text{nm}$; $\lambda_{em} = 598\,\text{nm}$) after growth for 7 h (logarithmic phase). The data are normalised to the cell density of the cell culture. (C) Quantification of biofilm formation using crystal violet (CV) (based on $\lambda_{max} = 550\,\text{nm}$). The data are normalised to the cell density of the planktonic cells in each sample (after growth for 24 h). (D) Characterisation of OMV particles formed by engineered $P.\ putida$ strains by determination of diameters (d) and the signal strength of count rates with DLS (see also Figure S7 showing a correlation of the sample concentration with signal intensity). Bars and DLS data are sorted in ascending order. Putative cellular localisation of proteins is indicated by different colours (OM: dark blue; PP: light blue; IM: orange; CP: yellow; unknown localisation: grey). Implemented manipulation of gene expression is indicated by arrows (empty arrows: up-regulation; filled arrows: down-regulation). ev (Ci): CRISPRi empty vector control; The data are mean values of independent triplicate measurements with their respective standard deviation. Significant differences in comparison to the untreated wild type are indicated by asterisks (determined by T-test; * $p \le 0.05$, ** $p \le 0.01$, *** $p \le 0.001$).

HIdE is a bifunctional enzyme involved in the biosynthesis of the LPS component L-glycero-D-mannoheptose (L,D-Hep) and localised in the cytoplasm, as reported for *E. coli* (Kneidinger et al., 2002; McArthur et al., 2005; Valvano et al., 2000). In a study with this organism, HIdE, together with other enzymes from LPS biosynthesis, was identified as involved in the formation of OMVs (Yang et al., 2021). MItA is a conserved lytic transglycosylase which is presumably

anchored in the OM and cleaves linkages between N-acetylglucosamine and N-acetylmuramic acid in the PG layer, thus far described for *E. coli* and *P. aeruginosa* (Chen et al., 2022; Lommatzsch et al., 1997; Mueller & Levin, 2020). PvdQ is a periplasmic (de)acetylase conserved in fluorescent Pseudomonads. In *P. putida* KT2440, it is involved in pyoverdine biosynthesis, where it catalyses the deacylation of the ferribactin precursor in the periplasm as

17517915, 2024, 1, Downloaded from https://ami-journals.onlinelibrary.wiley.com/doi/10.1111/1751-7915.14312 by Forschungszentrum Jülich GmbH Research Center, Wiley Online Library on [30/01/2024]. See the Terms and Conditions

and-conditions) on Wiley Online Library for rules of use; OA articles are governed by the applicable Creative Commons License

a maturation step to release the peptide from the IM (Koch et al., 2010; Ringel & Brüser, 2018).

Engineered vesiculation can help to improve the production of diverse natural products

Our results suggested that hypervesiculation could support biosynthetic compound production by P. putida KT2440. To verify this hypothesis, we chose the tripyrrolic compound prodigiosin (1), the indolocarbazoles violacein (2), and deoxyviolacein (3) that are co-produced by the respective biosynthetic pathway, phenazine-1-carboxylic acid (PCA) (4), and the carotenoid zeaxanthin (5). These are all relatively hydrophobic but chemically rather diverse bioactive compounds, for which previously characterised P. putida KT2440-derived production strains (and product analysis assays) were readily available. The expression vectors to up- or down-regulate the expression of the identified genes PP 2087, ethA, hldE, mltA and pvdQ were introduced in the four previously constructed strains P. putida pig21, vio12, PCA1, and crtΔX, which carried the respective biosynthetic gene clusters in the genome where they were constitutively expressed (Domröse et al., 2017; Loeschcke et al., 2013). Compound production was assessed by spectrophotometry or HPLC-PDA analyses (see Figure 6).

Production titres of the natural compounds increased to different levels depending on the used engineered producer strain. While for violaceins and zeaxanthin, a smaller increase of titres was observed upon manipulation of some target genes, prodigiosin and PCA titres were more clearly enhanced. Interestingly, this overall trend is not correlated with the hydrophobicity of the compounds (logP values: prodigiosin=4.07; violacein=1.88; deoxyviolacein=2.24; PCA=1.79; zeaxanthin=10.91; calculated by XLOGP3 software (Cheng et al., 2007)).

Previous reports on membrane or vesicle association of some compounds might explain the overall trends in parts: It is known that the final reaction of prodigiosin biosynthesis occurs at the membrane, and the release of prodigiosin or related structures by vesicles or unknown mechanisms has been suggested (Domröse et al., 2015; Matsuyama et al., 1986; Schrempf & Merling, 2015; Tan et al., 2020). A transporter has not yet been described. Similarly, release of violacein via OMVs has been described (Batista et al., 2020; Choi et al., 2020). Phenazines also end up in the culture broth of producing bacteria via unknown mechanisms (Bator et al., 2020; Jin et al., 2015; Sakhtah et al., 2016; Schmitz et al., 2015; Sporer et al., 2018). To our knowledge, a membrane association is not known. In contrast, carotenoids like zeaxanthin are thought to be associated with whole cells and to span the lipid double layer (Gruszecki & Strzałka, 2005). In this context, we evaluated the distribution of compounds between

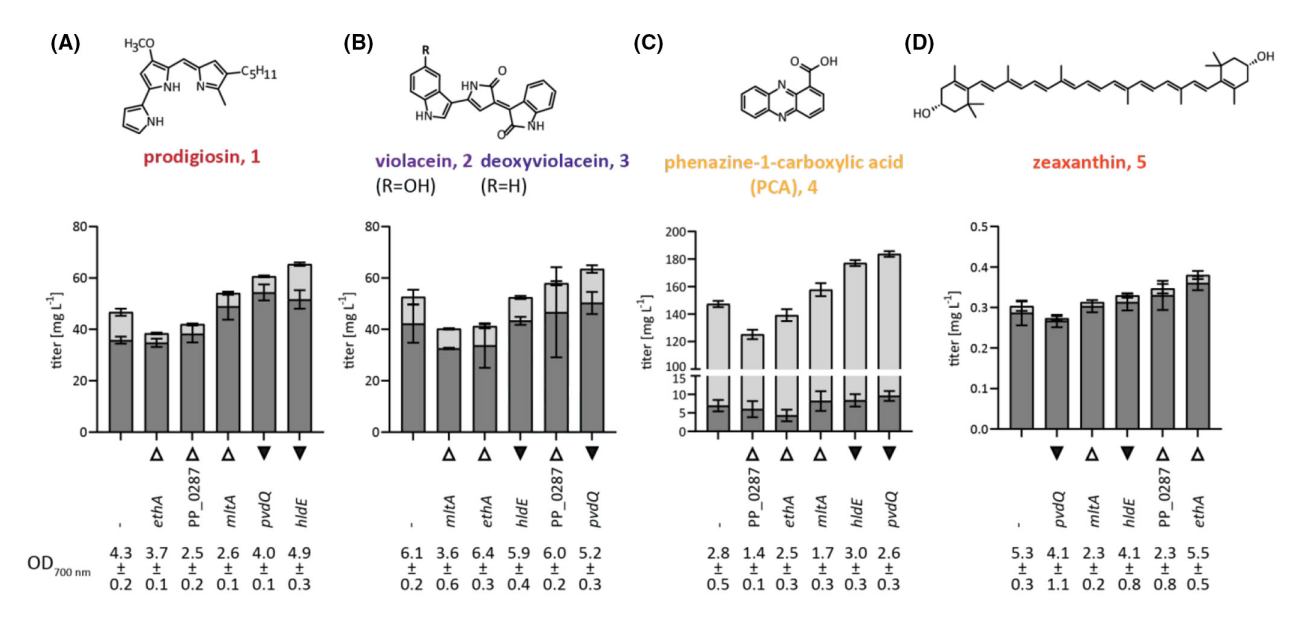


FIGURE 6 Recombinant natural compound production by *Pseudomonas putida* engineered for OMV release. Natural product titres were determined after extraction from both pellet fraction (dark grey) and supernatant (light grey) of the engineered *P. putida* strains (genetic targets addressed by up- (empty arrows) or down-regulation (filled arrows) are indicated) and compared to the respective producer strains (indicated as '-'). (A) Prodigiosin (1) produced by *P. putida* pig21. (B) Violacein (2)/deoxyviolacein (3) produced by *P. putida* vio12. (C) PCA (4) produced by *P. putida* PCA1. (D) Zeaxanthin (5) produced by *P. putida* crt \(\Delta \). Implemented manipulation of gene expression is indicated by arrows (empty arrows: up-regulation; filled arrows: down-regulation). Bars are sorted in ascending order. Cell densities reached at the end of the cultivation (after 48 h) are given below graphs. The data are mean values of independent triplicate measurements with their respective standard deviation.

17517915, 2024, 1, Downloaded from https://ami-journals.online/thrary. wiley.com/doi/10.1111/1751-7915.14312 by Forschungszentrum/Juitch CambH Research Center, Wiley Online Library on [30/01/2024]. See the Terms and Conditions (https://online/hibrary.wiley.com/terms-and-conditions) on Wiley Online Library for rules of use O.A articles are governed by the applicable Center, Wiley Online Library for rules of use O.A articles are governed by the applicable Center wiley.

the supernatant and cell pellet fractions. Here, we observed that vesiculation did not exclusively support the accumulation of compounds in the OMV-containing supernatant fraction, but that the engineered strains showed an increase of compound levels also in the cell pellet fraction (see Figure 6). However, we cannot exclude that OMVs may also be present in the cell pellet fraction.

The specific genetic manipulations had rather differential effects: While expression of ethA led to enhanced titres only in the zeaxanthin producer, repression of pvdQ increased those of all other products. In the prodigiosin producer, hldE repression was most effective. An increase in vesiculation upon manipulation of these targets (hldE, pvdQ, and ethA) in the production strains was verified by MADLS analysis (see Figure S11). The effect was not very pronounced in all cases, which might be due to the fact that the production can already cause relatively strong vesiculation (as demonstrated for prodigiosin, see Figure 1 and Table S1). OMV formation might be naturally limited by lipid supply and cellular integrity. Since excessive vesiculation must perturb cell envelope integrity, we tested cell viability by propidium iodide (PI) staining and found the engineered cells to be more damaged (see Figure S12). This indicates that vesiculation engineering may require careful finetuning for each case in order to achieve best results.

Notably, some of the engineered strains also did not reach the same cell densities as the parental production strains, which influenced the titres in the cultures (see Figure 6). Therefore, in terms of product yields [mg per gDCW], the manipulations had a higher (by up to 1.5- to 3-fold) and in parts a different effect (see Figure S13).

Our findings did not reveal a single outstanding genetic target which would allow improving production of all compounds. This cannot be expected as also suggested by findings reported for membrane engineering with E. coli (Yang et al., 2021). Differential effects may be caused, for example, by the temporal dynamics of vesiculation and biosyntheses. It was interesting to note that the ratio of violacein/deoxyviolacein was slightly changed by the manipulations (see Figure S14). Compared to the parental strain, cell pellet extracts of the manipulated strains showed a decrease of deoxyviolacein relative to violacein (except for pvdQ repression). Compared to these samples, supernatant extracts showed an increase in the relative deoxyviolacein levels (except for ethA expression). This might indicate that the more hydrophobic compound deoxyviolacein is more amenable to being excreted or to accumulate in vesicles.

Apart from optimising compound release by vesiculation, limitations in the biosynthetic pathways must also be considered. An example is zeaxanthin biosynthesis which is limited by the pool of available precursors (Hernandez-Arranz et al., 2019; Sánchez-Pascuala et al., 2019). Concerted efforts encompassing metabolic engineering and a fine-tuned engineering of the host tolerance shall boost production yields and allow to implement the biosynthetic production of highly toxic compounds which would otherwise be inaccessible.

CONCLUSION

In summary, we show that OMV formation is a natural response of P. putida KT2440 not only to external chemical stressors but also to the production of small molecules. Moreover, we demonstrate that this phenotype can be genetically engineered, which can improve production yields. In the future, the engineering of OMV formation may help to create robust chassis strains and serve as a potential tool to improve hitherto limited yields of natural products for biotechnological applications.

AUTHOR CONTRIBUTIONS

Nora Lisa Bitzenhofer: Conceptualisation (equal); data curation (lead); formal analysis (lead); methodology (equal); validation (lead); visualisation (lead); writing original draft (lead); writing – review and editing (equal). Carolin Höfel: Investigation (supporting); writing – review and editing (equal). Stephan Thies: Conceptualisation (supporting); funding acquisition (equal); validation (equal); writing - review and editing (equal). Andrea Jeanette Weiler: Investigation (supporting); methodology (supporting); resources (supporting); writing review and editing (equal). Christian Eberlein: Data curation (equal); formal analysis (equal); investigation (equal); writing – review and editing (equal). Hermann J. Heipieper: Data curation (equal); formal analysis (equal); resources (equal); writing - review and editing (equal). Renu Batra-Safferling: Data curation (equal); formal analysis (equal); resources (equal); writing - review and editing (equal). Pia Sundermeyer: Investigation (equal); methodology (equal); writing – review and editing (equal). Thomas Heidler: Investigation (equal); methodology (equal); writing - review and editing (equal). Carsten Sachse: Data curation (equal); formal analysis (equal); resources (equal); writing - review and editing (equal). Tobias Busche: Data curation (equal); formal analysis (equal); methodology (equal); writing - review and editing (equal). Jörn Kalinowski: Data curation (equal); formal analysis (equal); resources (equal); writing - review and editing (equal). Thomke Belthle: Investigation (equal); methodology (equal); writing - review and editing (equal). Thomas Drepper: Formal analysis (equal); supervision (equal); writing - review and editing (equal). Karl-Erich Jaeger: Funding acquisition (equal); writing original draft (equal); writing - review and editing (equal). Anita Loeschcke: Conceptualisation (equal); data curation (equal); formal analysis (equal); funding acquisition (equal); supervision (lead); validation (equal); writing original draft (equal); writing – review and editing (equal).

The authors gratefully acknowledge the support given by Dr. Manuel Banzhaf by discussions about the cell envelope. For support regarding DLS analysis, we acknowledge Dr. Annette Eckhardt from X-Tal Concepts. We thank Esther Knieps-Grünhagen for supporting preparative column chromatography of prodigiosin and Vera Svensson for support in density gradient centrifugation. This work was supported by the German Federal Ministry of Education and Research via the project NO-STRESS under grant numbers 031B0852B (to N.L.B., S.T., A.L. and K.-E.J.) and 031B085C (to C.E. and H.J.H.), as well as the projects GlycoX/161B0866A (to S.T., A.L. and K.-E.J.) and LipoBiocat/031B0837A (to S.T. and K.-E.J.). The authors gratefully acknowledge support by the "European Regional Development Fund (EFRE)" through project "Cluster Industrial Biotechnology (CLIB) Kompetenzzentrum Biotechnologie (CKB)" (34.EFRE-0300095/1703FI04) for T. Busche and J. Kalinowski and by the Deutsche Forschungsgemeinschaft (DFG, German Research Foundation) - Project ID 458090666/CRC1535/1 (A.J.W. and T.D.). Open Access funding enabled and organized by Projekt DEAL.

FUNDING INFORMATION

No funding information provided.

CONFLICT OF INTEREST STATEMENT

The authors declare that there are no competing interests associated with the manuscript.

DATA AVAILABILITY STATEMENT

Transcriptomic data are available at the ArrayExpress database (www.ebi.ac.uk/arrayexpress) under accession no. E-MTAB-12470. All data are available upon request.

ORCID

Nora Lisa Bitzenhofer b https://orcid. org/0000-0002-2790-4929 Carolin Höfel https://orcid. org/0000-0002-4230-2942 Stephan Thies https://orcid. ora/0000-0003-4240-9149 Christian Eberlein https://orcid. org/0000-0003-4521-8145 Hermann J. Heipieper lo https://orcid. org/0000-0002-3723-9600 Renu Batra-Safferling https://orcid. org/0000-0002-8597-4335 Thomas Heidler https://orcid. org/0000-0002-5997-3945 Carsten Sachse https://orcid. org/0000-0002-1168-5143

REFERENCES

- Askitosari, T.D., Boto, S.T., Blank, L.M. & Rosenbaum, M.A. (2019) Boosting heterologous phenazine production in *Pseudomonas* putida KT2440 through the exploration of the natural sequence space. *Frontiers in Microbiology*, 10, 1–12.
- Atashgahi, S., Sánchez-Andrea, I., Heipieper, H.J., van der Meer, J.R., Stams, A.J.M. & Smidt, H. (2018) Prospects for harnessing biocide resistance for bioremediation and detoxification. *Science*, 360, 743–746.
- Avila-Calderón, E.D., Ruiz-Palma, M.d.S., Aguilera-Arreola, M.G., Velázquez-Guadarrama, N., Ruiz, E.A., Gomez-Lunar, Z. et al. (2021) Outer membrane vesicles of gram-negative bacteria: an outlook on biogenesis. Frontiers in Microbiology, 12, 557902.
- Batianis, C., Kozaeva, E., Damalas, S.G., Martín-Pascual, M., Volke, D.C., Nikel, P.I. et al. (2020) An expanded CRISPRi toolbox for tunable control of gene expression in *Pseudomonas putida*. *Microbial Biotechnology*, 13, 368–385.
- Batista, J.H., Leal, F.C., Fukuda, T.T.H., Alcoforado Diniz, J., Almeida, F., Pupo, M.T. et al. (2020) Interplay between two quorum sensing-regulated pathways, violacein biosynthesis and VacJ/Yrb, dictates outer membrane vesicle biogenesis in Chromobacterium violaceum. Environmental Microbiology, 22, 2432–2442.
- Bator, I., Wittgens, A., Rosenau, F., Tiso, T. & Blank, L.M. (2020) Comparison of three xylose pathways in *Pseudomonas putida* KT2440 for the synthesis of valuable products. *Frontiers in Bioengineering and Biotechnology*, 7, 1–18.
- Bauman, S.J. & Kuehn, M.J. (2006) Purification of outer membrane vesicles from *Pseudomonas aeruginosa* and their activation of an IL-8 response. *Microbes and Infection*, 8, 2400–2408.
- Baumgarten, T., Sperling, S., Seifert, J., von Bergen, M., Steiniger, F., Wick, L.Y. et al. (2012) Membrane vesicle formation as a multiple-stress response mechanism enhances *Pseudomonas putida* DOT-T1E cell surface hydrophobicity and biofilm formation. *Applied and Environmental Microbiology*, 78, 6217–6224.
- Belda, E., van Heck, R.G.A., José Lopez-Sanchez, M., Cruveiller, S., Barbe, V., Fraser, C. et al. (2016) The revisited genome of *pseudomonas putida* KT2440 enlightens its value as a robust metabolic *chassis*. *Environmental Microbiology*, 18, 3403–3424.
- Beuttler, H., Hoffmann, J., Jeske, M., Hauer, B., Schmid, R.D., Altenbuchner, J. et al. (2011) Biosynthesis of zeaxanthin in recombinant *Pseudomonas putida*. *Applied Microbiology and Biotechnology*, 89, 1137–1147.
- Bitto, N.J., Zavan, L., Johnston, E.L., Stinear, T.P., Hill, A.F. & Kaparakis-Liaskos, M. (2021) Considerations for the analysis of bacterial membrane vesicles: methods of vesicle production and quantification can influence biological and experimental outcomes. *Microbiology Spectrum*, 9, 1–15.
- Bitzenhofer, N.L., Kruse, L., Thies, S., Wynands, B., Lechtenberg, T., Rönitz, J. et al. (2021) Towards robust *Pseudomonas* cell factories to harbour novel biosynthetic pathways. *Essays in Biochemistry*, 65, 319–336.
- Blanco, P., Hernando-Amado, S., Reales-Calderon, J., Corona, F., Lira, F., Alcalde-Rico, M. et al. (2016) Bacterial multidrug efflux pumps: much more than antibiotic resistance determinants. *Microorganisms*, 4, 14.

- Bligh, E.G. & Dyer, W.J. (1959) A rapid method of total lipid extraction and purification. *Canadian Journal of Biochemistry and Physiology*, 37, 911–917.
- Blum, M., Chang, H.-Y., Chuguransky, S., Grego, T., Kandasaamy, S., Mitchell, A. et al. (2021) The InterPro protein families and domains database: 20 years on. *Nucleic Acids Research*, 49, 344–354.
- Bösl, B., Grimminger, V. & Walter, S. (2006) The molecular chaperone Hsp104—a molecular machine for protein disaggregation. *Journal of Structural Biology*, 156, 139–148.
- Calero, P., Jensen, S.I., Bojanovič, K., Lennen, R.M., Koza, A. & Nielsen, A.T. (2018) Genome-wide identification of tolerance mechanisms toward *p* -coumaric acid in *Pseudomonas putida*. *Biotechnology and Bioengineering*, 115, 762–774.
- Chen, Y.-C., Kalawong, R., Toyofuku, M. & Eberl, L. (2022) The role of peptidoglycan hydrolases in the formation and toxicity of *Pseudomonas aeruginosa* membrane vesicles. *microLife*, 3, 1–9
- Cheng, T., Zhao, Y., Li, X., Lin, F., Xu, Y., Zhang, X. et al. (2007) Computation of octanol-water partition coefficients by guiding an additive model with knowledge. *Journal of Chemical Information and Modeling*, 47, 2140–2148.
- Choi, S.Y., Lim, S., Cho, G., Kwon, J., Mun, W., Im, H. et al. (2020) Chromobacterium violaceum delivers violacein, a hydrophobic antibiotic, to other microbes in membrane vesicles. Environmental Microbiology, 22, 705–713.
- Cook, T.B., Jacobson, T.B., Venkataraman, M.V., Hofstetter, H., Amador-Noguez, D., Thomas, M.G. et al. (2021) Stepwise genetic engineering of *Pseudomonas putida* enables robust heterologous production of prodigiosin and glidobactin a. *Metabolic Engineering*, 67, 112–124.
- Deng, M. & Misra, R. (1996) Examination of AsmA and its effect on the assembly of *Escherichia coli* outer membrane proteins. *Molecular Microbiology*, 21, 605–612.
- Domröse, A., Hage-Hülsmann, J., Thies, S., Weihmann, R., Kruse, L., Otto, M. et al. (2019) Pseudomonas putida rDNA is a favored site for the expression of biosynthetic genes. Scientific Reports, 9, 7028.
- Domröse, A., Klein, A.S., Hage-Hülsmann, J., Thies, S., Svensson, V., Classen, T. et al. (2015) Efficient recombinant production of prodigiosin in *Pseudomonas putida*. Frontiers in Microbiology, 6, 972.
- Domröse, A., Weihmann, R., Thies, S., Jaeger, K.-E., Drepper, T. & Loeschcke, A. (2017) Rapid generation of recombinant *Pseudomonas putida* secondary metabolite producers using yTREX. *Synthetic and Systems Biotechnology*, 2, 310–319.
- Eberlein, C., Baumgarten, T., Starke, S. & Heipieper, H.J. (2018) Immediate response mechanisms of gram-negative solvent-tolerant bacteria to cope with environmental stress: *cis-trans* isomerization of unsaturated fatty acids and outer membrane vesicle secretion. *Applied Microbiology and Biotechnology*, 102, 2583–2593.
- Eberlein, C., Starke, S., Doncel, Á.E., Scarabotti, F. & Heipieper, H.J. (2019) Quantification of outer membrane vesicles: a potential tool to compare response in *Pseudomonas putida* KT2440 to stress caused by alkanols. *Applied Microbiology* and *Biotechnology*, 103, 4193–4201.
- Florez, C., Raab, J.E., Cooke, A.C. & Schertzer, J.W. (2017) Membrane distribution of the *Pseudomonas* quinolone signal modulates outer membrane vesicle production in *Pseudomonas* aeruginosa. MBio, 8, 1–13.
- Gruszecki, W.I. & Strzałka, K. (2005) Carotenoids as modulators of lipid membrane physical properties. *Biochimica et Biophysica Acta (BBA) Molecular Basis of Disease*, 1740, 108–115.
- Hanahan, D. (1983) Studies on transformation of *Escherichia coli* with plasmids. *Journal of Molecular Biology*, 166, 557–580.

- Hartl, F.U., Bracher, A. & Hayer-Hartl, M. (2011) Molecular chaperones in protein folding and proteostasis. *Nature*, 475, 324–332.
- Heipieper, H.J., Diefenbach, R. & Keweloh, H. (1992) Conversion of cis unsaturated fatty acids to trans, a possible mechanism for the protection of phenol-degrading Pseudomonas putida P8 from substrate toxicity. Applied and Environmental Microbiology, 58, 1847–1852.
- Heipieper, H.J., Loffeld, B., Keweloh, H. & de Bont, J.A.M. (1995)
 The *cis/trans* isomerisation of unsaturated fatty acids in *Pseudomonas putida* S12: an indicator for environmental stress due to organic compounds. *Chemosphere*, 30, 1041–1051.
- Heipieper, H.J., Meinhardt, F. & Segura, A. (2003) The *cis-trans* isomerase of unsaturated fatty acids in *Pseudomonas* and *Vibrio*: biochemistry, molecular biology and physiological function of a unique stress adaptive mechanism. *FEMS Microbiology Letters*, 229, 1–7.
- Henderson, P.J.F., Maher, C., Elbourne, L.D.H., Eijkelkamp, B.A., Paulsen, I.T. & Hassan, K.A. (2021) Physiological functions of bacterial "multidrug" efflux pumps. *Chemical Reviews*, 121, 5417–5478.
- Hernandez-Arranz, S., Perez-Gil, J., Marshall-Sabey, D. & Rodriguez-Concepcion, M. (2019) Engineering *Pseudomonas putida* for isoprenoid production by manipulating endogenous and shunt pathways supplying precursors. *Microbial Cell Factories*, 18, 152.
- Hilker, R., Stadermann, K.B., Schwengers, O., Anisiforov, E., Jaenicke, S., Weisshaar, B. et al. (2016) ReadXplorer 2—detailed read mapping analysis and visualization from one single source. *Bioinformatics*, 32, 3702–3708.
- Hogenkamp, F., Hilgers, F., Bitzenhofer, N.L., Ophoven, V., Haase, M., Bier, C. et al. (2022) Optochemical control of bacterial gene expression: novel photocaged compounds for different promoter systems. *Chembiochem*, 23, e202100467.
- Jin, K., Zhou, L., Jiang, H., Sun, S., Fang, Y., Liu, J. et al. (2015) Engineering the central biosynthetic and secondary metabolic pathways of *Pseudomonas aeruginosa* strain PA1201 to improve phenazine-1-carboxylic acid production. *Metabolic Engineering*, 32, 30–38.
- Juodeikis, R. & Carding, S.R. (2022) Outer membrane vesicles: biogenesis, functions, and issues. *Microbiology and Molecular Biology Reviews*, 86, e0003222.
- Klimentová, J. & Stulík, J. (2015) Methods of isolation and purification of outer membrane vesicles from gram-negative bacteria. *Microbiological Research*, 170, 1–9.
- Kneidinger, B., Marolda, C., Graninger, M., Zamyatina, A., McArthur, F., Kosma, P. et al. (2002) Biosynthesis pathway of ADP-I-glycero-β-d- *manno* -heptose in *Escherichia coli. Journal of Bacteriology*, 184, 363–369.
- Koch, G., Jimenez, P.N., Muntendam, R., Chen, Y., Papaioannou, E., Heeb, S. et al. (2010) The acylase PvdQ has a conserved function among fluorescent *Pseudomonas* spp. *Environmental Microbiology Reports*, 2, 433–439.
- Kulp, A. & Kuehn, M.J. (2010) Biological functions and biogenesis of secreted bacterial outer membrane vesicles. *Annual Review of Microbiology*, 64, 163–184.
- Langmead, B. & Salzberg, S.L. (2012) Fast gapped-read alignment with Bowtie 2. Nature Methods, 9, 357–359.
- Levine, T.P. (2019) Remote homology searches identify bacterial homologues of eukaryotic lipid transfer proteins, including Chorein-N domains in TamB and AsmA and Mdm31p. *BMC Molecular and Cell Biology*, 20, 43.
- Li, H., Handsaker, B., Wysoker, A., Fennell, T., Ruan, J., Homer, N. et al. (2009) The sequence alignment/map format and SAMtools. *Bioinformatics*, 25, 2078–2079.
- Lin, B. & Tao, Y. (2017) Whole-cell biocatalysts by design. *Microbial Cell Factories*, 16, 106.

17517915, 2024, 1, Downloaded from https://ami-journals

onlinelibrary.wiley.com/doi/10.1111/1751-7915.14312 by Forschungszentrum Jülich GmbH Research Center, Wiley Online Library on [30/01/2024]. See the Terms

on Wiley Online Library for rules of use; OA articles are governed by the applicable Creative Commons License

- Loeschcke, A., Markert, A., Wilhelm, S., Wirtz, A., Rosenau, F., Jaeger, K-E. et al. (2013) TREX: a universal tool for the transfer and expression of biosynthetic pathways in bacteria. *ACS Synthetic Biology*, 2, 22–33. Available from: https://doi.org/10.1021/sb3000657
- Loeschcke, A. & Thies, S. (2015) *Pseudomonas putida*—a versatile host for the production of natural products. *Applied Microbiology and Biotechnology*, 99, 6197–6214.
- Loeschcke, A. & Thies, S. (2020) Engineering of natural product biosynthesis in *Pseudomonas putida*. *Current Opinion in Biotechnology*, 65, 213–224.
- Lommatzsch, J., Templin, M.F., Kraft, A.R., Vollmer, W. & Höltje, J.V. (1997) Outer membrane localization of murein hydrolases: MltA, a third lipoprotein lytic transglycosylase in *Escherichia coli. Journal of Bacteriology*, 179, 5465–5470.
- Love, M.I., Huber, W. & Anders, S. (2014) Moderated estimation of fold change and dispersion for RNA-seq data with DESeq2. *Genome Biology*, 15, 550.
- Makra, I., Terejánszky, P. & Gyurcsányi, R.E. (2015) A method based on light scattering to estimate the concentration of virus particles without the need for virus particle standards. *MethodsX*, 2. 91–99.
- Mashburn, L.M. & Whiteley, M. (2005) Membrane vesicles traffic signals and facilitate group activities in a prokaryote. *Nature*, 437, 422–425.
- Mashburn-Warren, L., Howe, J., Brandenburg, K. & Whiteley, M. (2009) Structural requirements of the *Pseudomonas* quinolone signal for membrane vesicle stimulation. *Journal of Bacteriology*, 191, 3411–3414.
- Matsuyama, T., Murakami, T., Fujita, M., Fujita, S. & Yano, I. (1986) Extracellular vesicle formation and biosurfactant production by Serratia marcescens. Microbiology, 132, 865–875.
- Mauger, M., Ferreri, C., Chatgilialoglu, C. & Seemann, M. (2021) The bacterial protective armor against stress: the *cis-trans* isomerase of unsaturated fatty acids, a cytochrome-c type enzyme. *Journal of Inorganic Biochemistry*, 224, 111564.
- McArthur, F., Andersson, C.E., Loutet, S., Mowbray, S.L. & Valvano, M.A. (2005) Functional analysis of the glycero-manno -heptose 7-phosphate kinase domain from the bifunctional HIdE protein, which is involved in ADP- I glycero d manno -heptose biosynthesis. *Journal of Bacteriology*, 187, 5292–5300.
- Minerdi, D., Zgrablic, I., Sadeghi, S.J. & Gilardi, G. (2012) Identification of a novel Baeyer-Villiger monooxygenase from Acinetobacter radioresistens: close relationship to the Mycobacterium tuberculosis prodrug activator EtaA. Microbial Biotechnology, 5, 700–716.
- Misra, R. & Miao, Y. (1995) Molecular analysis of *asmA*, a locus identified as the suppressor of OmpF assembly mutants of *Escherichia coli* K-12. *Molecular Microbiology*, 16, 779–788.
- Molina-Santiago, C., Cordero, B.F., Daddaoua, A., Udaondo, Z., Manzano, J., Valdivia, M. et al. (2016) *Pseudomonas putida* as a platform for the synthesis of aromatic compounds. *Microbiology*, 162, 1535–1543.
- Morrison, W.R. & Smith, L.M. (1964) Preparation of fatty acid methyl esters and dimethylacetals from lipids with boron fluoride—methanol. *Journal of Lipid Research*, 5, 600–608.
- Mozaheb, N. & Mingeot-Leclercq, M.-P. (2020) Membrane vesicle production as a bacterial defense against stress. Frontiers in Microbiology, 11, 60221.
- Mueller, E.A. & Levin, P.A. (2020) Bacterial cell wall quality control during environmental stress. MBio, 11, 1–15.
- Nelson, K.E., Weinel, C., Paulsen, I.T., Dodson, R.J., Hilbert, H., Martins dos Santos, V.A.P. et al. (2002) Complete genome sequence and comparative analysis of the metabolically versatile Pseudomonas putida KT2440. Environmental Microbiology, 4, 799–808.
- Nicolaou, S.A., Gaida, S.M. & Papoutsakis, E.T. (2010) A comparative view of metabolite and substrate stress and tolerance

- in microbial bioprocessing: from biofuels and chemicals, to biocatalysis and bioremediation. *Metabolic Engineering*, 12, 307–331.
- Nikel, P.I. & de Lorenzo, V. (2018) Pseudomonas putida as a functional chassis for industrial biocatalysis: from native biochemistry to trans-metabolism. Metabolic Engineering, 50, 142–155.
- O'Toole, G.A. (2011) Microtiter dish biofilm formation assay. *Journal of Visualized Experiments*, 47, e2437.
- Prior, J.E., Lynch, M.D. & Gill, R.T. (2010) Broad-host-range vectors for protein expression across gram negative hosts. *Biotechnology and Bioengineering*, 106, 326–332.
- Qi, L.S., Larson, M.H., Gilbert, L.A., Doudna, J.A., Weissman, J.S., Arkin, A.P. et al. (2013) Repurposing CRISPR as an RNAguided platform for sequence-specific control of gene expression. Cell, 152, 1173–1183.
- Rehdorf, J., Kirschner, A. & Bornscheuer, U.T. (2007) Cloning, expression and characterization of a Baeyer-Villiger monooxygenase from *Pseudomonas putida* KT2440. *Biotechnology Letters*, 29, 1393–1398.
- Ringel, M.T. & Brüser, T. (2018) The biosynthesis of pyoverdines. *Microbial Cell*, 5, 424–437.
- Roca, A., Rodríguez-Herva, J.-J., Duque, E. & Ramos, J.L. (2008) Physiological responses of *Pseudomonas putida* to formalde-hyde during detoxification. *Microbial Biotechnology*, 1, 158–169.
- Rodrigues, A.L., Göcke, Y., Bolten, C., Brock, N.L., Dickschat, J.S. & Wittmann, C. (2012) Microbial production of the drugs violacein and deoxyviolacein: analytical development and strain comparison. *Biotechnology Letters*, 34, 717–720.
- Rodriguez, B.V. & Kuehn, M.J. (2020) Staphylococcus aureus secretes immunomodulatory RNA and DNA via membrane vesicles. Scientific Reports, 10, 18293.
- Roier, S., Zingl, F.G., Cakar, F., Durakovic, S., Kohl, P., Eichmann, T.O. et al. (2016) A novel mechanism for the biogenesis of outer membrane vesicles in gram-negative bacteria. *Nature Communications*, 7, 10515.
- Rouvière, P.E., De Las Peñas, A., Mecsas, J., Lu, C.Z., Rudd, K.E. & Gross, C.A. (1995) *rpoE*, the gene encoding the second heat-shock sigma factor, sigma E, in *Escherichia coli*. *The EMBO Journal*, 14, 1032–1042.
- Sakhtah, H., Koyama, L., Zhang, Y., Morales, D.K., Fields, B.L., Price-Whelan, A. et al. (2016) The *Pseudomonas aeruginosa* efflux pump MexGHI-OpmD transports a natural phenazine that controls gene expression and biofilm development. *Proceedings of the National Academy of Sciences of the United States*, 113, E3538–E3547.
- Sambrook, J., Fritsch, E. & Maniatis, T. (1989) *Molecular cloning: a laboratory manual*. New York: Cold Sprin Habor Laboratory Press, p. 545.
- Sánchez-Pascuala, A., Fernández-Cabezón, L., de Lorenzo, V. & Nikel, P.I. (2019) Functional implementation of a linear glycolysis for sugar catabolism in *Pseudomonas putida*. *Metabolic Engineering*, 54, 200–211.
- Schmitz, S., Nies, S., Wierckx, N., Blank, L.M. & Rosenbaum, M.A. (2015) Engineering mediator-based electroactivity in the obligate aerobic bacterium *Pseudomonas putida* KT2440. *Frontiers in Microbiology*, 6, 1–13.
- Schrempf, H. & Merling, P. (2015) Extracellular Streptomyces lividans vesicles: composition, biogenesis and antimicrobial activity. Microbial Biotechnology, 8, 644–658.
- Schwanemann, T., Otto, M., Wierckx, N. & Wynands, B. (2020) Pseudomonas as versatile aromatics cell factory. Biotechnology Journal, 15, 1900569.
- Schwechheimer, C. & Kuehn, M.J. (2015) Outer-membrane vesicles from gram-negative bacteria: biogenesis and functions. *Nature Reviews. Microbiology*, 13, 605–619.
- Schwechheimer, C., Sullivan, C.J. & Kuehn, M.J. (2013) Envelope control of outer membrane vesicle production in gram-negative bacteria. *Biochemistry*, 52, 3031–3040.

- Sporer, A.J., Beierschmitt, C., Bendebury, A., Zink, K.E., Price-Whelan, A., Buzzeo, M.C. et al. (2018) Pseudomonas aeruginosa PumA acts on an endogenous phenazine to promote self-resistance. Microbiology, 164, 790-800.
- Tan, D., Fu, L., Sun, X., Xu, L. & Zhang, J. (2020) Genetic analysis and immunoelectron microscopy of wild and mutant strains of the rubber tree endophytic bacterium Serratia marcescens strain ITBB B5-1 reveal key roles of a macrovesicle in storage and secretion of prodigiosin. Journal of Agricultural and Food Chemistry, 68, 5606-5615.
- Tan, S.Z., Reisch, C.R. & Prather, K.L.J. (2018) A robust CRISPR interference gene repression system in Pseudomonas. Journal of Bacteriology, 200, e00575-17.
- Tan, Z., Yoon, J.M., Nielsen, D.R., Shanks, J.V. & Jarboe, L.R. (2016) Membrane engineering via trans unsaturated fatty acids production improves Escherichia coli robustness and production of biorenewables. Metabolic Engineering, 35, 105-113.
- Tu, Q., Yin, J., Fu, J., Herrmann, J., Li, Y., Yin, Y. et al. (2016) Room temperature electrocompetent bacterial cells improve DNA transformation and recombineering efficiency. Scientific Reports, 6, 24648.
- Valvano, M.A., Marolda, C.L., Bittner, M., Glaskin-Clay, M., Simon, T.L. & Klena, J.D. (2000) The rfaE gene from Escherichia coli encodes a bifunctional protein involved in biosynthesis of the lipopolysaccharide core precursor ADP- I - glycero - d - manno -heptose. Journal of Bacteriology, 182, 488-497.
- Van Bogaert, I.N.A., Groeneboer, S., Saerens, K. & Soetaert, W. (2011) The role of cytochrome P450 monooxygenases in microbial fatty acid metabolism. FEBS Journal, 278, 206-221.
- Weimer, A., Kohlstedt, M., Volke, D.C., Nikel, P.I. & Wittmann, C. (2020) Industrial biotechnology of Pseudomonas putida: advances and prospects. Applied Microbiology and Biotechnology, 104. 7745-7766.
- Winsor, G.L., Griffiths, E.J., Lo, R., Dhillon, B.K., Shay, J.A. & Brinkman, F.S.L. (2016) Enhanced annotations and features for comparing thousands of Pseudomonas genomes in the

- Pseudomonas genome database. Nucleic Acids Research, 44, D646-D653
- Xiong, X., Deeter, J.N. & Misra, R. (1996) Assembly-defective OmpC mutants of Escherichia coli K-12. Journal of Bacteriology, 178, 1213-1215.
- Yang, D., Park, S.Y. & Lee, S.Y. (2021) Production of rainbow colorants by metabolically engineered Escherichia coli. Advanced Science, 8, 2100743.
- Yu, H., Lu, Y., Lan, F., Wang, Y., Hu, C., Mao, L. et al. (2023) Engineering outer membrane vesicles to increase extracellular electron transfer of Shewanella oneidensis. ACS Synthetic Biology, 12, 1645-1656.
- Zhang, J.J., Tang, X., Zhang, M., Nguyen, D. & Moore, B.S. (2017) Broad-host-range expression reveals native and host regulatory elements that influence heterologous antibiotic production in gram-negative bacteria. MBio, 8, e01291-17.

SUPPORTING INFORMATION

Additional supporting information can be found online in the Supporting Information section at the end of this article.

How to cite this article: Bitzenhofer, N.L., Höfel, C., Thies, S., Weiler, A.J., Eberlein, C., Heipieper, H.J. et al. (2024) Exploring engineered vesiculation by Pseudomonas putida KT2440 for natural product biosynthesis. Microbial Biotechnology, 17, e14312. Available from: https://doi.org/10.1111/1751-7915.14312